# CALIBRATION OF A VON HAMOS SPECTOMETER FOR X-RAY SOURCE MONITORING

Capstone Project Report for

Physics 492R

by

Michael Johnson

Submitted to the Department of Physics and Astronomy in partial fulfillment

of graduation requirements for the degree of

Bachelor of Science

Brigham Young University

April 2006

## Abstract

Applications such as x-ray microscopy and lithography need x-ray sources that have well-defined emission spectra. A 533 nm beam from a frequency doubled 1064 nm laser strikes a solid target creates a plasma with emissions in the soft x-ray range. A von Hamos spectrometer using a cylindrically bent mica crystal and a linear CCD array detector is used to monitor the x-ray emission spectrum. The spectrometer is calibrated for wavelength using a Mg spectrum with known characteristic lines. The intensity scale is calibrated using a pin diode of known calibration.

## Acknowledgements

I would like to give special thanks to Brigham Young University, the Department of Physics and Astronomy, and Dr. Larry Knight for their generous support of this project. I also appreciate my fellow student collaborators, Tyler Weeks, Matt Harrison, and Nathan Packard for their constant assistance. I also would like to thank Dr. Alexander Shevelko of the Lebedev Physical Insititute in Moscow for his powerful guidance and direction. I appreciate immensely the others that helped us with this project when Dr. Knight was out of the country, specifically Dr. Scott Bergeson and especially John Elsworth, who took on extra work to keep us going and gave us much needed daily guidance and help. Finally, I thank Dr. Matthew Asplund for allowing us to work in his lab and giving us help and support there.

**CONTENTS**


**1. Introduction** 1

1.1 Laser-produced Plasma Sources 1

1.2 Lithography 1

1.3 Lithography Requirements 2

**2. Methods** 3

2.1. Von Hamos Spectrometer 3

2.2. Experimental Setup 4

2.3. Plasma Production 5

2.4. Alignment 7

2.5. Wavelength Calibration 9

2.6. Intensity Calibration 11

**3. Results and Discussion** 13

3.1 Emission Instabilities 13

3.2 Calibrated Spectra 15

**4. Conclusions** 17

## LIST OF FIGURES


| | | |
|---|---|---|
| 1. | Lithography | 1 |
| 2. | Von Hamos Spectrometer Design | 3 |
| 3. | Experimental Setup | 4 |
| 4. | Target Assembly | 5 |
| 5. | Focal Spot Size | 6 |
| 6. | Uncalibrated Spectrum | 7 |
| 7. | Step Filter | 8 |
| 8. | Diffraction Pattern | 9 |
| 9. | Bragg Diffraction | 10 |
| 10. | Quasi-monochromatic X-ray Source | 11 |
| 11. | Relative Electron Temperature | 13 |
| 12. | Relative X-ray Yield | 14 |
| 13. | Calibrated Magnesium Spectrum | 15 |
| 14. | Calibrated Copper Spectrum | 16 |
| 15. | Calibrated Zinc Spectrum | 16 |

# 1. Introduction

## 1.1 Laser Produced Plasma X-ray Sources

Researchers are working to develop laser-produced plasmas as x-ray sources for various applications such as x-ray microscopy and lithography [1,2]. Laser-produced plasmas show promise because of their ability to provide high-brightness x-rays at a low cost compared to other sources such as synchrotron rings or z-pinch devices [3]. In the research project discussed in this work, emissions from such laser produced plasmas were monitored by calibrating a spectrometer which can characterize spectra in the soft x-ray range. This wavelength range is of special interest for x-ray lithography.

## 1.2 Lithography

Lithography is the process where light passes through a mask to expose an image on a substrate, and the exposed areas can then be chemically etched away to leave the desired features (see Figure 1). Historically, optical light has been the main tool of lithography, but the desire for features smaller than 100 nanometers is pushing optical

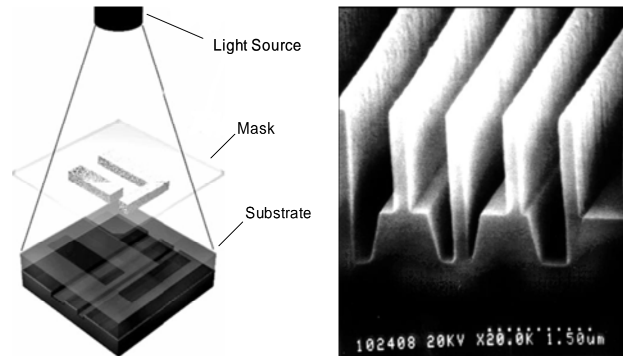


**Figure 1. Lithography.** This figure shows the basic components of a lithography system and an example of an etching with nanometer scale features. From reference [4].

lithography to its limit [5]. Researchers are developing methods for ultraviolet and x-ray lithography that would allow the industry to continue printing features smaller than 100 nanometers.

### 1.3 Lithography Requirements

X-ray lithography has the capability of printing features of the desired size, but it also has strict requirements about the wavelength, uniformity, and intensity of the x-rays that would be used. It is estimated [6] that for x-ray lithography to be feasible, the source would have to deliver 15 $mJ/cm^2$ in a 1.3 s exposure interval with less than a 1% variation from uniformity over a 3x3 $cm^2$ area of the substrate. The optimum wavelengths should occupy a 20% bandwidth around 1.2 nm. The demands illustrated by these requirements indicate the need to develop well-characterized laser-produced plasma x-ray sources and monitor their emission spectra and intensities.

Other work is being done to develop laser-produced plasma x-ray sources that are bright enough to meet the intensity and uniformity requirements. JMAR has developed an x-ray collimator to permit the x-rays to reach the lithography mask uniformly [7]. They have also developed a powerful laser that appears to be capable of delivering the required x-ray flux [8]. Their work also shows that debris damage to lithography equipment can be considerably reduced by using copper tape as a target in a helium gas environment [8].

These advances are promising, and an instrument that provides accurate monitoring of the x-ray spectral intensity will aid in ensuring that the application

requirements are met. This research has focused on developing a spectrometer to monitor the wavelength and intensity emissions from laser-produced plasmas. V. Boiko et. al. [9] state that spectroscopy is an effective tool for diagnostics of plasmas. This work shows the response to the need to have well-defined sources by calibrating a von Hamos spectrometer that can be used to monitor the x-ray emissions. This effort has demonstrated that such a spectrometer can be used to give the intensity in absolute units of a given wavelength in the emission spectrum.

# 2. Methods

## 2.1 Von Hamos Spectrometer

The instrument developed is a spectrometer after the von Hamos design, which is advantageous because of its focusing geometry [10]. In the von Hamos scheme, the diffraction crystal is bent into a cylinder, and the x-ray source and detector are placed on the axis of the cylinder (see figure 2). Emissions from the source (which must

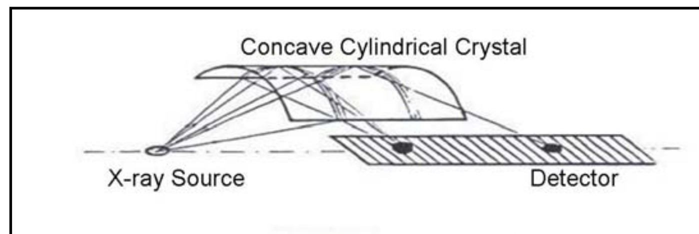


**Figure 2. Von Hamos Spectrometer Design.** Mica crystal is bent into a cylindrical shape and the x-ray source and detector are placed on the axis. From reference [11].

approximate a point-source) are then refracted by the crystal and focused back onto a line on the cylinder axis. This design has the advantage over a flat crystal spectrometer design because there is a higher intensity incident on the detector, and it consequently has a higher resolving power [12].

Mica is used as the crystal for the spectrometer because it is capable of bending to relatively small diameters, 20 mm in this case. The cylindrical geometry was achieved by bending the mica crystal around the outside of a brass cylindrical casing through which a window was cut to allow radiation from a source to have a direct path to the mica. Mica has a 2d spacing of 19.88 Angstroms which allows a view of emissions in the wavelength range of interest—around 10 Angstroms.

A Toshiba CCD linear array was used as the detector. Because the wavelengths of interest are in the soft x-ray range, which are highly absorbed by most materials, the glass cover of the CCD had to be removed. The detector was positioned on the axis of the cylinder in a capsule that fits into the cylindrical brass casing.

## 2.2 Experimental Setup

The complete spectrometer devise was then integrated into the setup shown in Figure 3. Because the wavelengths of interest are in the soft x-ray region which are

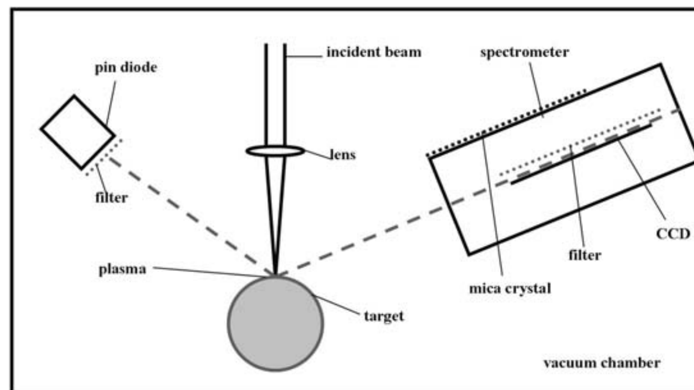


**Figure 3. Experimental Setup.** The incident laser beam generates a plasma which emits x-rays collected by a pin diode and a spectrometer.

highly absorbed by matter, all measurements had to be done in a vacuum chamber. The laser entered the chamber through a window and was focused by a converging lens onto a solid target to produce a plasma. The x-ray emissions from the plasma were recorded by

a pin diode and the spectrometer.  The other individual components of the setup and their functions are described in more detail later in this work.

## 2.3 Plasma Production

The first step in monitoring x-ray emissions was to create a laser-produced plasma.  The laser was a commercial model from Coherent capable of delivering 400 mJ per pulse at its first harmonic of 1064 nm.  To increase x-ray conversion efficiency [13], a doubling crystal was used to pulse the laser at 532 nm at energies of around 200 mJ per pulse.  The laser has a 3 ns pulse, which delivers a power of $6x10^7$ Watts per pulse.  The beam entered a vacuum chamber through a window and was focused onto the target by a converging lens with a focal length of 5 cm.

The target was a solid cylinder mounted on a micron screw driven by a Mycom five-lead stepper motor as shown in Figure 4.  The motor was synchronized with the laser

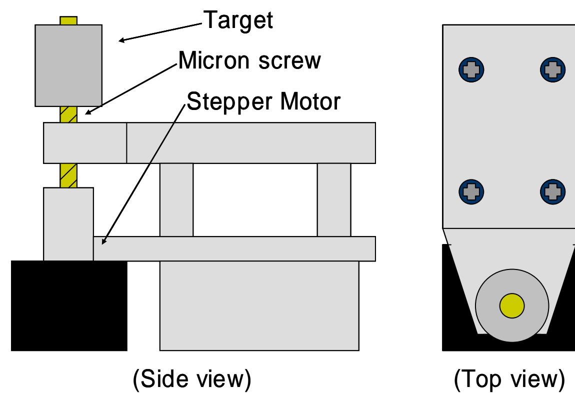


**Figure 4. Target assembly.** The motor turns the screw after each laser shot, exposing a clean surface of the cylindrical target to the incident beam, keeping all instruments aligned.

pulse so that the target rotated slightly with each laser shot, exposing a new surface to the incoming beam.  This allowed the instruments to remain aligned with each new laser shot by keeping the x-ray source in the same location. The target material was readily changed

by replacing it with a new cylinder, or by covering the cylinder with a foil of a different substance.

The spot size was calculated by positioning a linear CCD array to be hit directly by the focused laser beam. The laser was pulsed at low power (25 mJ) and attenuated by several filters to avoid damaging the CCD. The position of the CCD was adjusted until it was located at the focal spot of the laser, with special care being taken to ensure that the CCD linear array was along the diameter of the focal spot. The output from the CCD in Figure 5 shows that approximately five pixels (FWHM) were being illuminated by the

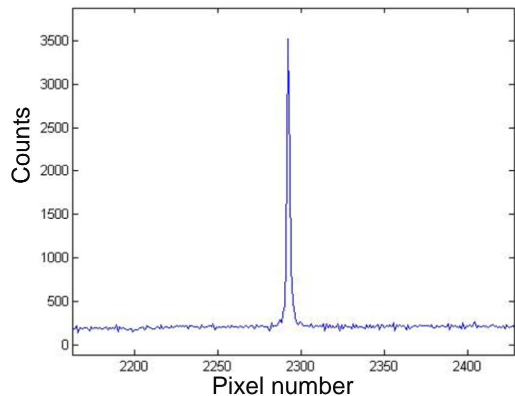


**Figure 5. Focal Spot Size.** The laser was focused onto the CCD, and the resulting peak indicates that five pixels were illuminated at FWHM.

laser light. Each pixel is 6 micrometers long with a 2 micrometer gap between them, giving a focal spot diameter of approximately 40 micrometers. Thus the laser is capable of delivering $5x10^{12}$ W/cm$^2$ to the target, ionizing the material to create a plasma.

As the plasma cools, it emits radiation which can be collected by the spectrometer. The electron temperature of the plasma created by this pulse can be determined [14] by observing the ratios of the resonance (w) and satellite (j+k) lines as shown in Figure 6. Dr. Shevelko developed a relationship for the characteristic

magnesium lines which was used to determine that the plasmas produced had electron temperatures between 200 and 250 eV.

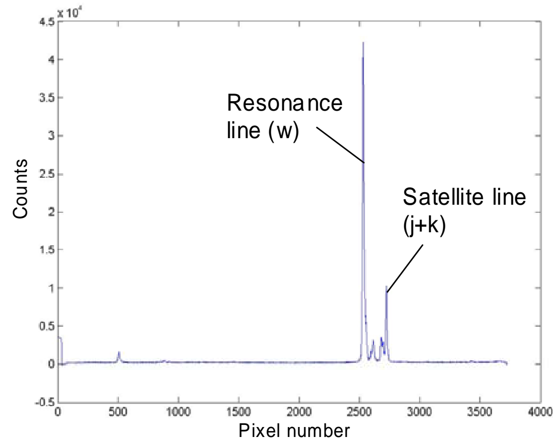


**Figure 6. Uncalibrated Spectrum** showing the resonance and satellite lines used to determine electron temperature.

## 2.4 Alignment

With the plasma being generated, the next step was to align the instruments. The alignment procedure for the spectrometer began with placing the CCD linear array detector on the axis of the cylindrical spectrometer. To accomplish this, a cylindrical CCD holder was designed that fits snugly into the brass spectrometer casing. The holder was designed so that the top plane of the CCD chip will rest on a plane running through the diameter of the cylinder (ensuring correct vertical position). The linear array in the horizontal plane was adjusted using four positioning screws in the CCD holder. The holder was placed in a microscope that has been calibrated with a guiding line to show the center line of the cylinder. The positioning screws were adjusted until the CCD linear array is in line with the cylindrical axis.

The CCD holder can be slid in and out of the spectrometer casing (towards or away from the source), which selects the wavelength range to be observed. Sliding the

detector towards the source allows a view of longer wavelengths while sliding it away from the source selects for shorter wavelengths.

The target position was adjusted until it was located at the focal spot of the laser. This was done by evacuating the chamber and maximizing the amount of x-rays produced. A CCD was placed in the chamber facing the x-ray source. The CCD was covered by a filter with different layer thicknesses of beryllium, aluminum, mylar, and copper. X-rays passing through the filter were attenuated to various degrees depending on the filter thickness at that point, and the step-like output from the CCD in Figure 7 was observed. The position of the lens is adjusted by remotely activating a picomotor connected to the transition stage on which the lens is attached. The lens is moved to the position where the CCD displays the most x-rays passing through the filter.

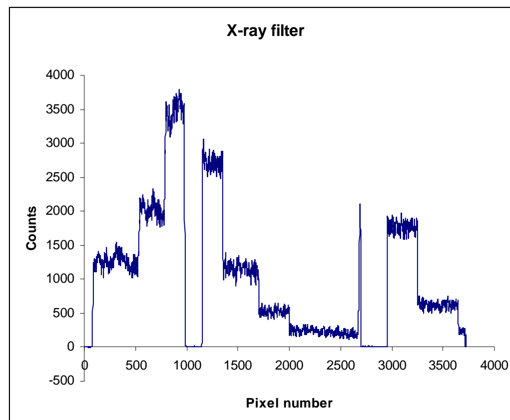


**Figure 7. Step filter**. X-rays passing through different thicknesses of materials are used to indicate the position for maximum x-ray production.

The next step in aligning the spectrometer involved ensuring that the cylindrical axis was in line with the x-ray source. This was accomplished by using the visible light at the source spot as a guide. The CCD in its holder was placed in the spectrometer casing, and the aluminum filter was removed to allow visible light to be detected by the CCD. The laser was attenuated by a frosted glass filter and struck a spot on the target

that had already been pocked by a high-power laser shot. The reflected visible light from this pock mark reflects again off the mica crystal of the spectrometer and gives a diffraction pattern on the CCD (see Figure 8). The spectrometer was mounted on a translation stage and the position was finely adjusted to alter the diffraction pattern on the

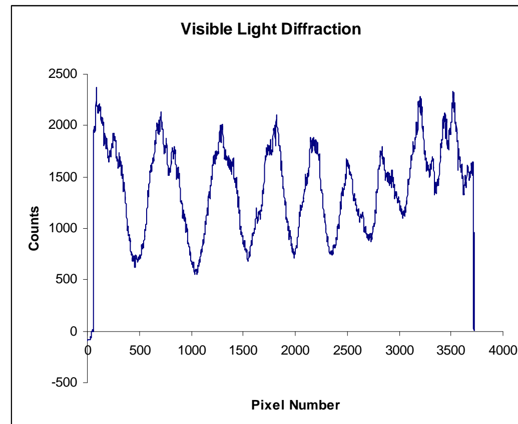


**Figure 8. Diffraction pattern.** A visible light diffraction pattern is used to align the spectrometer by maximizing the peaks.

CCD. The source was aligned with the axis of the cylinder when the diffraction pattern was optimized to display the highest peaks and troughs.

## 2.5 Wavelength Calibration

With the spectrometer properly aligned, the calibration of the wavelength scale had to be performed. This portion of the calibration of the spectrometer followed a method outlined by R. Whitlock, et. al. [15], where the wavelengths detected by the spectrometer were referenced to several known emission lines. A relation to calibrate the unknown wavelengths was determined using the geometry of the setup and Bragg diffraction. Figure 9 shows the relevant geometry of the spectrometer for the wavelength calibration process.

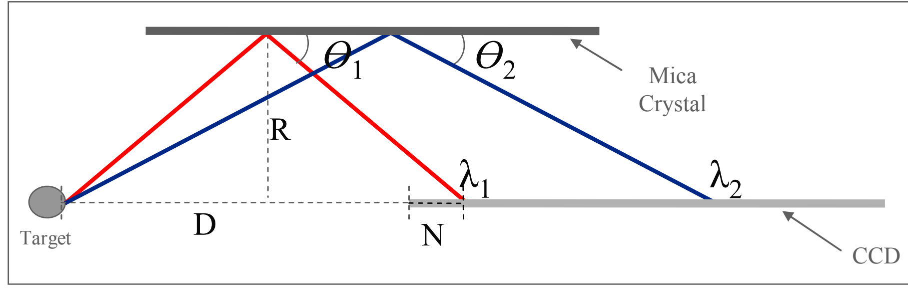


**Figure 9. Bragg diffraction.** The geometry associated with Bragg diffraction relevant to the spectrometer is shown.

The total distance $L$ from the source to where the line shows up on the CCD is

$$L = D + N = 2R\cot(\theta) \qquad (1)$$

where $D$ is the distance form the source to the first pixel on the CCD, $N$ is the distance from the first pixel of the CCD to the position on the CCD where the wavelength was detected, $R$ is the radius of curvature of the crystal, and $\theta$ is the Bragg angle. The Bragg diffraction equation is

$$n\lambda = 2d\sin(\theta) \qquad (2)$$

where $n$ is the diffraction order, $\lambda$ is the wavelength, $d$ is the lattice spacing, and $\theta$ is the Bragg angle. Solving (1) for $\theta$ and substituting it in to (2) yields

$$\lambda = \frac{2d}{n}\sin\left\{\cot^{-1}\left(\frac{D+N}{2R}\right)\right\} \quad (3).$$

The $2d$ spacing is known, and the distance $N$ is a function of pixel number: the pixel number multiplied by the length of each pixel (8μm for this CCD). Thus yielding an equation that relates the wavelength to the pixel number $N$, the distance of the CCD from the source $D$, and the radius of curvature $R$.

When the spectrum obtained for magnesium was observed, the wavelengths of several lines were determined by comparison to spectra obtained in the literature [16, 17]. These known lines were then associated with the CCD pixel number at which they

appeared.  The unknowns in equation (3) were then only *R* and *D*.  By using two known lines, two versions of equation (3) were solved simultaneously to discover the values for *D* and *R*.  This method contained an inherent validity check when *R* is compared to the expected value of the radius of the cylinder, which was 20 mm.  Once *D* and *R* were known, equation (3) then gave the wavelength as a function of pixel number, which was applied to the whole linear array.

## 2.6 Intensity Calibration

The next major aspect of the research was to calibrate the intensity scale.  This was done using a commercially calibrated pin diode and comparing its output to that of the spectrometer.  This method of calibration becomes straightforward if the diode and spectrometer are both restricted to viewing the same x-ray wavelengths, which might seem difficult to achieve with the relatively limited spectral range of the spectrometer. However, this criteria was met by using a specific combination of target material and filters to create a quasi-monochromatic x-ray source [18].  In this case, an aluminum filter was used in conjunction with a magnesium target.  The emissions from the magnesium with wavelengths below the K-edge of the aluminum were filtered, passing only a few characteristic lines to be detected by the CCD and the diode (see Figure 10).

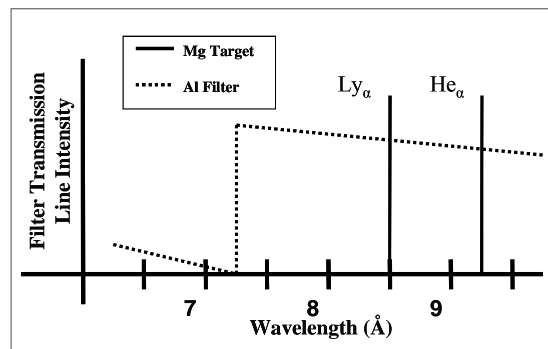


**Figure 10. Quasi-monochromatic x-ray source.** Using an aluminum target and a magnesium filter ensures that both the pin diode and the spectrometer are viewing the same wavelengths.

The pin diode was connected to a digital oscilloscope that could read and record the output from a single pulse. The laser beam created a plasma with x-ray emissions, and the outputs from the pin diode and the CCD were read simultaneously. The intensity calibration was then performed by relating the intensity recorded by the spectrometer to the known intensity determined from the diode.

The pin diode was used to calculate the known intensity emitted from the source in units of photons per steradian. The oscilloscope output from the pin diode showed a decay, from which the time constant τ was determined. Using the known resistance of the pin diode, the capacitance was obtained from the relation $\tau = RC$, and the number of charge carriers was then calculated from $Q = CV$. The quantum efficiency of the diode was given by the manufacturer, and thus the number of charge carriers was used to determine how many x-ray photons were incident on the diode. The size of the diode detection surface and its distance from the source were then used to calculate the solid angle and to get the intensity of the source in photons per steradian.

Using this knowledge of the intensity from the source, the intensity scale of the spectrometer was calibrated. The solid angle subtended by the illuminated portion of the spectrometer crystal was then calculated. The total number of counts from the spectrometer was integrated and associated with the total number of photons from the source for the corresponding solid angle subtended by the spectrometer to give the number of photons per count. The spectrometer then gave the number of photons per steradian at each pixel.

# 3. Results and Discussion

## 3.1 Emission Instabilities

Several magnesium spectra were analyzed to determine the stability of the x-ray source. The x-ray intensity incident to the CCD detector was integrated, and the total intensity was plotted verses laser energy for several shots in Figure 11. There was a relationship between the x-ray output and the laser power used to generate the plasma, though there was some instability.

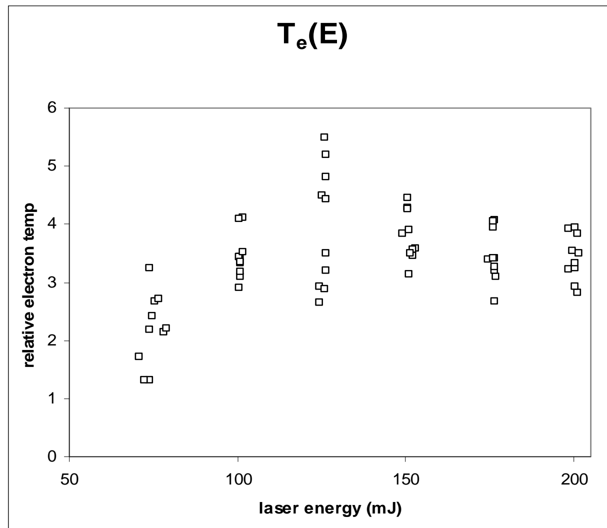


**Figure 11.** The relative electron temperature as a function of laser energy shows a trend, but there is still significant uncertainty.

Another interesting phenomenon occurs when the electron temperature of the plasma is considered. The electron temperature of the plasma was determined for several shots and plotted against the x-ray yield in Figure 12, giving a random distribution of data points.

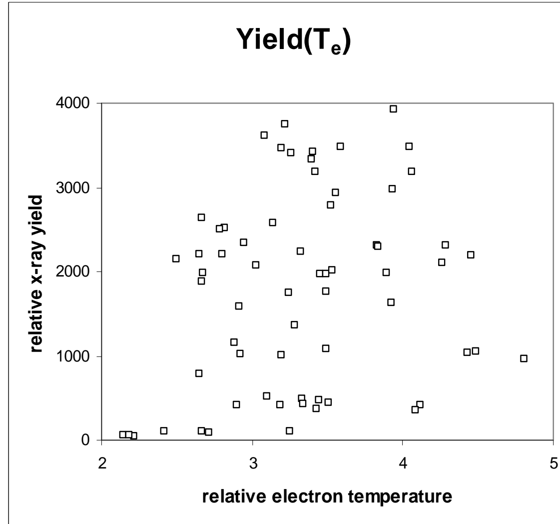


**Figure 12.** The relative x-ray yield vs. relative electron temperature gives a random distribution indicating the need to monitor the x-ray yield.

These observations bring up a question concerning the stability of the x-ray source. One possible explanation for these instabilities is that the beam quality was very poor. This was indicated by the obvious hot spots when observing the beam profile, and also by comparing the measured spot size to the calculated spot size. The measured value for the spot size was known, but it could also be determined from the equation [2]

$$\varphi = 1.22N\left(\frac{f}{\phi}\right)\lambda \quad (4)$$

where $\varphi$ is the focal spot diameter, $N$ is a measure of the beam quality, $f$ is the focal length of the lens, $\phi$ is the entering beam diameter, and $\lambda$ is the wavelength. For this equation to hold true for the measured spot size, $N$ would be approximately 350, where a good quality beam would have $N$ on the order of unity.

Whatever the reasons, there were definite instabilities in the x-ray yield which would need to be monitored to ensure that the laser-produced plasma was meeting the requirements for its application. The von Hamos spectrometer was able to detect these

instabilities.  Once the spectrometer is calibrated, it can give a shot-to-shot measurement of the x-ray spectral yield.

### 3.2 Calibrated Spectra

Calibrated spectra were obtained for plasmas from Mg, Cu, and Zn targets, which are shown in Figures 13, 14, and 15 respectively.

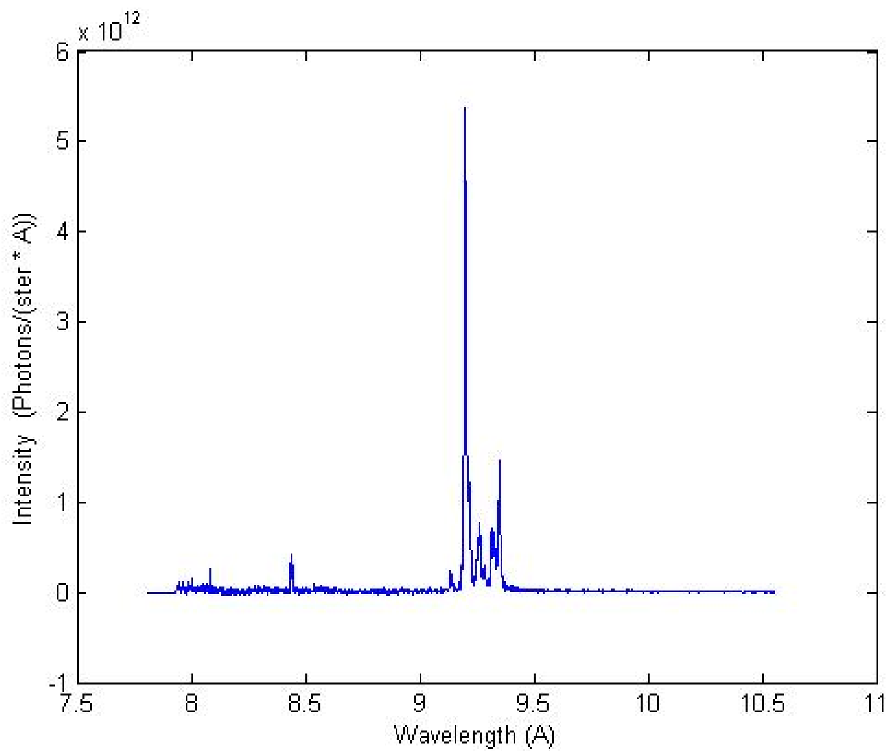


**Figure 13.** Calibrated magnesium spectrum.

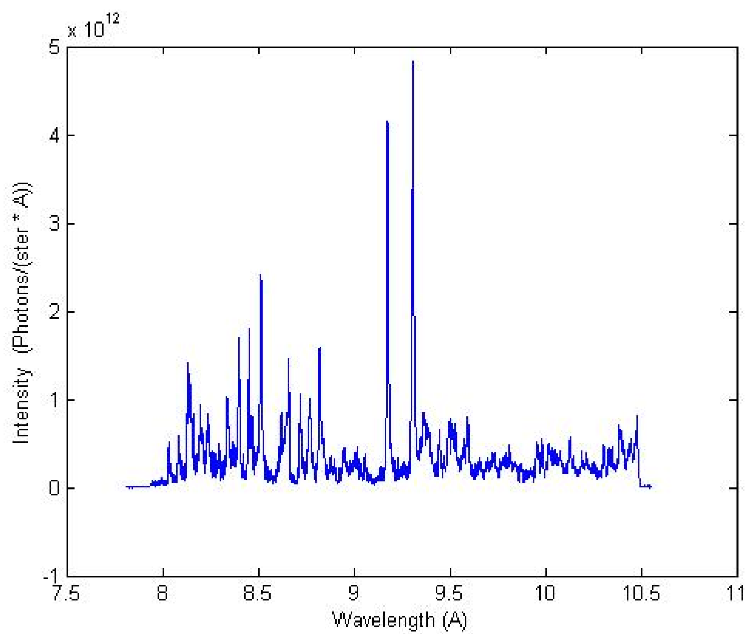


**Figure 14.** Calibrated copper spectrum.

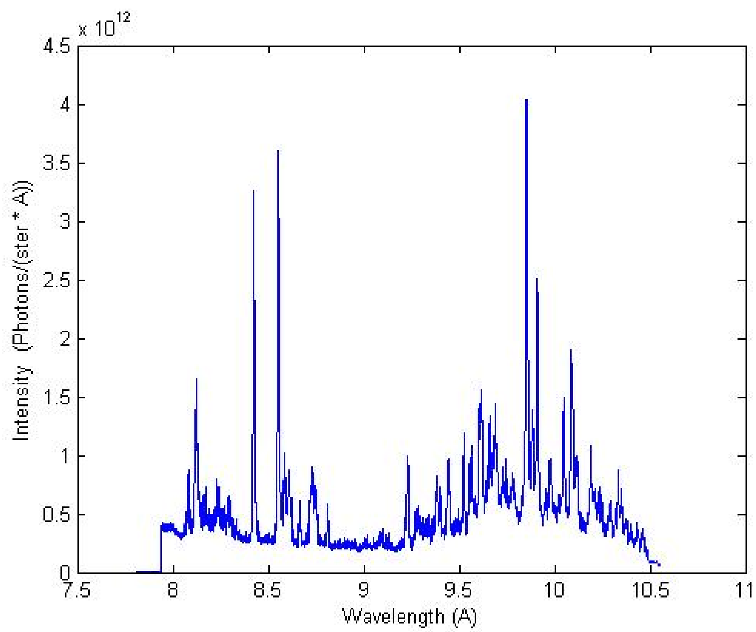


**Figure 15.** Calibrated zinc spectrum.

# 4. Conclusions

A focusing spectrometer of the von Hamos design was calibrated to display spectra in absolute units. This device shows promise in monitoring laser-produced plasma x-ray sources for applications such as x-ray lithography where there are stringent x-ray source requirements. The spectrometer was shown to detect instabilities in the shot-to-shot emission spectra.

It would be possible to develop a computer program that would allow real-time monitoring of the x-ray source emissions.

Future work includes performing similar calibration of a conical spectrometer. The advantage of the conical design is that the device can be placed farther from the source to view the desired wavelength range. This would be beneficial because it would allow other instruments (such as collimators) to be placed close to the source. Being further from the source would also reduce the debris damage to the crystal.

# References


[1] Georg Soumagne, et. al, “Emission spectra of laser-produced plasmas for EUV and soft x-ray sources,” Proc. SPIE, **5482**(26) (2004).

[2] I.C.E. Turcu, et. al, “Microfocus Soft x-ray source generated by a compact high power laser-plasma,” Proc. SPIE, **4144**(1) (2000).

[3] N. Economou, D. Flanders, “Prospects for high-brightness x-ray sources for lithography,” J. Vac. Sci. Technol. **19**(868) (1981).

[4] F. Cerina, “X-ray imaging: applications to patterning and lithography,” J. Phys. D: Appl. Phys. **33** (2000).

[5] R. Forber, et. al, “High power laser-produced plasma source for nano-lithography,” Proc. SPIE, **5196**(97) (2004).

[6] P. Celliers, L. B. DaSilva, C. B. Dane, S. Mrowka, M. Norton, L. Hackel, D. Matthews J. R. Maldonado, and J. A. Abate, “Optimization of x-ray sources from a high average power ND:Glass laser-produced plasma for proximity lithography,” ICF Annual Report. pp. 157-167 (1995).

[7] R. Forber, et. al, “Collimated point-source x-ray nanolithography,” J. Vac. Sci. Technol. B **20**(6) (2002).

[8] I.C.E. Turcu, et. al, “High power x-ray point source for next generation lithography,” Proc. SPIE, **3767**(21) (1999).

[9] V. A. Boiko, A. Ya. Faenov, S. A. Pikuz, “X-ray spectroscopy of multiply charged ions from laser plasmas,” J. Quant. Spectrosc. Radiat. Transfer, **19** (1978).

[10] A. Shevelko, L. Knight, Q. Wang, O. Yakushev, “Absolute x-ray calibration of laser-produced plasmas using a CCD linear array and a focusing crystal spectrometer,” Proc. SPIE, **4504**(215) (2001).

[11] A. Shevelko, “X-ray spectroscopy of laser-produced plasmas using a von Hamos spectrograph,” Proc. SPIE, **3406**(91) (1998).

[12] P. Beiersdorfer, et. al, “Very high resolution soft x-ray spectrometer for an electron beam ion trap,” Rev. Sci. Instrum. **68**(1) (1997).

[13] W. Mead, et. al, “Laser irradiation of disk targets at 0.53 μm wavelength,” Phys. Fluids, **26**(8) (1983).

[14] A. Vinogradov, I. Skobelev, E. Yukov, "Determination of plasma density from spectra of heliumlike ions," Sov. J. Quant. Electron., **5**(6) (1975).

[15] R. Whitlock, et. al, "X-ray spectral measurements of the JMAR high power laser-plasma source," Proc. SPIE, **4781**(35) (2002).

[16] L. Presnyakov, "X-ray spectroscopy of high-temperature plasma," Sov. Phys. Usp., **19**(5) (1976).

[17] L. Vainshtein, U. Safronova, A. Urnov, "Dielectric satellites of multiply-charged ions resonance lines," Proceedings of P. N. Lebedev Physical Institute, Nova Science, Ed. N. Basov, **119** (1980).

[18] A. Shevelko, I. Beigman, L. Knight, "Formation of quasi-monochromatic soft x-ray radiation from laser-produced plasmas," Proc. SPIE, **4787**(11) (2002).